16th Australasian Fluid Mechanics Conference
Crown Plaza, Gold Coast, Australia
2-7 December 2007

Driving Cell Seeding Using Surface Acoustic Wave Fluid Actuation

Haiyan Li,[1] James R. Friend[1] and Leslie Y. Yeo[1]

[1] Micro/Nanophysics Research Laboratory,
Monash University, VIC, 3800 AUSTRALIA

Abstract

In this paper, we investigate the ability to drive fluid streaming via a surface acoustic wave (SAW) into a porous bioscaffold structure, and to exploit this effect to deliver fluorescent particles/yeast cells into the scaffold as a potential rapid and efficient method for cell seeding in tissue engineering. The results demonstrate that the seeding process takes approximately 10 seconds, much shorter than that if the cell suspension were to perfuse through the scaffold under the effects of gravity alone (approximately 30 mins). By increasing the input power, both the velocity of the fluid flow and the particle seeding efficiency can be enhanced. At 560 mW, fluid velocities of the order 10 mm/s were achieved; in this case, the particle/yeast seeding efficiency is around 92%. In addition to rapid seeding, the SAW streaming-induced perfusion is observed to significantly improve the uniformity of the scaffold cell distribution due to greater penetration into the scaffold. Finally, we verify using a methylene violet staining procedure that 80% of the yeast cells seeded by the SAW method within the scaffold remained viable.

1. Introduction

A SAW is analogous to an earthquake wave propagating along the surface with an amplitude of a few nanometers. The SAW is created by an interdigital transducer electrode [1]. The wavelength and resonance frequency of the SAW is defined by the width of each individual finger along the wave propagation direction and the gap between them; the amplitude of the SAW, on the other hand, is determined by the amplitude of the applied electrical signal. Different IDT and substrate designs can generate different forms of SAW. In this work, we make use of a Rayleigh wave, which is an axial-surface-normal polarized SAW [2]. SAW technology has been developed for the use of biotechnology, including mixing, bioparticle manipulation and pathogen detection in microfluidic devices [3–5]. When in contact with a liquid drop placed above the SAW substrate, bulk liquid recirculation is induced within the drop through a process known as acoustic streaming [6]. Essentially, the SAW is diffracted at the Rayleigh angle θ_R into the fluid as it propagates beneath the drop. For an infinite half space, θ_R is given by the ratio of the sound velocities in the substrate and in the fluid, respectively. It has been shown that the SAW can induce a free drop to translate along the direction of the SAW propagation if the intensity of the acoustic radiation component into the fluid is sufficiently high [4]. Based on this mechanism, a technology for transporting a free droplet on a microfluidic device without any mechanically moving components can be developed [4].

The broad mandate of tissue engineering is the generation of new tissue or organs for repairing damaged ones by culturing cells on a biocompatible and biodegradable porous scaffold. The desired cells have first to be seeded into the scaffold while at the same time limiting any denaturing or lysing that could potentially render the cells ineffective [7]. In addition, the uniformity of the cell distribution within the scaffold and the efficiency of the seeding process determine the homogeneity and efficiency of the newly generated tissue. Highly efficient cell seeding processes can yield substantial savings in cost and improvement in cell viability by reducing adverse effects on cells, thus leading to improved cell adhesion, proliferation and differentiation [8].

Since most of the scaffolds used for tissue engineering are hydrophobic and porous with small pore sizes (typically 10-150 μm), perfusion of the cell suspension into the scaffold in the absence of external driving forces is exceptionally slow due to the large capillary resistance. Under gravity-driven perfusion, which we shall henceforth refer to as the *static seeding* method, seeding times are roughly between hours to days. Nevertheless, this method has traditionally been employed in the past due to its simplicity [9-11]. Besides long seeding times, non-uniform cell distributions within the scaffold are also typical. This is due to the inability of the cell suspension to penetrate deep within the scaffold due to the large capillary resistance; most cells are therefore seeded only along the periphery of the scaffold surface. For example, with static seeding, it has been found that new bone tissue forms easily at the scaffold surface but to a much lesser extent at the centre of the scaffold [11, 12].

In this work, we demonstrate a novel method for rapidly and efficiently driving a suspension containing synthetic particles and yeast cells into a polymer scaffold for tissue engineering applications through SAW actuation [13].

2. Materials and Methods

2.1 Scaffolds

Scaffolds were prepared using a conventional solvent casting-particulate leaching method [14] using poly-caprolactone (PCL, MW = 65,000, MP = 65°C) (Sigma Chemical Co., USA). The porosity of the scaffold was about 90% ± 1.5%, as determined by using Archimedes' principle [15].

2.2 Fluorescent particles and yeast cell source

An aqueous suspension of 5 μm green fluorescent polystyrene (PS) microspheres (Duke Scientific Corporation, USA) was first employed to allow visualisation of the seeding process and to determine the spatial distribution of the seeded particles in the scaffold. The excitation and emission maxima wavelengths for these particles are 468 nm (blue) and 508 nm (green), respectively. These PS microparticles were obtained in the form of a 1% (weight/volume) aqueous suspension, containing 1.4×10^8 particles/ml. In the experiment, the original suspension was diluted with deionised (DI) water to a concentration of 1.4×10^6 particles/ml.

Yeast stock cultures consisting of 1% yeast extract, 0.5% neutralized bacteriological peptone and 1% glucose solidified with 1.5% agar (weight/volume) were maintained on standard agar. All media were autoclaved immediately after preparation at 121°C and 15 psi for 15 min. Yeast cells were grown aerobically to the required cell density at room temperature.

2.3 Seeding techniques

A SAW is generated by transmitting a radio frequency (RF) signal to one of the interdigital transducers (IDT) fabricated onto a piezoelectric substrate. The IDT essentially converts the applied

RF signal into a SAW, which travels from the IDT in both directions along the substrate surface and perpendicular to the direction of the strip electrodes with low divergence. Here, an 0.5 mm thick, 127.68°YX cut, X-propagating lithium niobate ($LiNbO_3$ or LN, Roditi, London UK) single crystal was used as the SAW substrate to generate a Rayleigh wave upon excitation of the IDT by an RF signal. A 4 nm titanium layer and a 150 nm aluminium layer were sputter-deposited upon this substrate. A standard alternating finger IDT with 60 straight finger pairs and an aperture of 8 mm was fabricated using photolithography; the strip and gap widths were 49 μm, thus giving a wavelength λ of 196 μm. The IDT was driven with a sinusoidal signal at the resonance frequency $f_0 = c/\lambda$, wherein c = 3788 m/s is the SAW velocity; thus, $f_0 \sim 19.35$ MHz.

Figure 1 shows a schematic of the experimental setup. The wires in contact with the bus bars of the input IDT are connected to the RF power source. A 20 μl drop containing the fluorescent PS particles with concentration 1.4×10^6 particles/ml is deposited onto the surface of the SAW device between the IDT and the scaffold. To observe the fluorescent PS particles, a high-speed video camera (Olympus iSpeed, Tokyo, Japan) was used together with a reflected fluorescent microscope system (Olympus BXFM, Tokyo, Japan) to monitor the dynamics of the seeding process. To excite the particle fluorescence, we employed wideband blue light with an intensity maximum at 468 nm.

For static seeding, a 20 μl drop of fluorescent particulate suspension with concentration 1.4×10^6 particles/ml was placed on the top surface of a PCL scaffold. The same observation system was used to monitor the seeding process. The approximate time required for the scaffold to completely perfuse into the droplet suspension until no liquid above the surface is apparently left, was determined through visual inspection using the microscope.

2.4 Image analysis

For image analysis, seeded scaffolds were cut perpendicularly to the long axis into six 1 mm thick slices. The cross-section of each slice was then observed under the reflected fluorescent microscope.

2.5 Particle seeding efficiency

Using the images acquired through the high-speed video capture, the velocity of the fluid flowing external to the scaffold was computed by dividing the distance that the drop suspension travelled prior to entry into the scaffold with the time taken. The influence of the input RF power on the suspension's velocity prior to entry into the scaffold and the particle seeding efficiency of the scaffolds were investigated. The particle seeding efficiency was evaluated according to the following: the SAW radiation was terminated when the entire suspension entered the scaffold completely, i.e., when no liquid external to the scaffold remained on the SAW surface. None of the liquid was permitted to circumvent the scaffold or to atomise by limiting the input power below that required for drop atomisation. The SAW substrate was

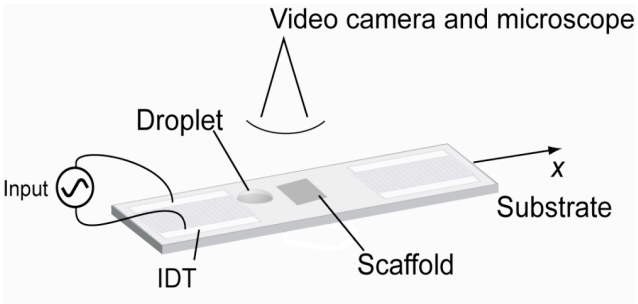

Figure 1 Schematic representation of the experimental setup for scaffold cell seeding method using SAW actuation.

then rinsed using DI water and the solution was collected. The number of fluorescent particles in this solution, N_1, was determined by using a haemocytometer (Hausser Scientific, Horsham, PA, Sigma, USA). The *particle seeding efficiency* of the scaffold is then

$$\textit{Particle seeding efficiency}\ (\%) = 100 \times (2.8\times10^4 - N_1) / 2.8\times10^4. \quad (1)$$

2.6 Yeast cell seeding efficiency and viability

The scaffold samples containing the yeast cells were allowed to dry at room temperature overnight. The dehydrated samples were then cut into six 1 mm thick slices and each slice was digested in 1 mL proteinase K (Sigma Chemical Co., USA) solution, prepared at a concentration of 1 mg/mL in 50 mM Tris, for 18 h at 56°C. To terminate the reaction, we used a proteinase K inhibitor, phenylmethylsulfonyl fluoride (PMSF, Sigma Chemical Co., USA). Aliquots of the digest for each section were subsequently analysed using the haemocytometer to obtain the cell concentration at each section ($C_a - C_f$). If the concentration of original seeding suspension is C_0 (1×10^8 cells/ml), the *cell seeding efficiency* in each section x is therefore

$$\textit{Cell seeding efficiency in each section}\ (\%) = 100(C_x/C_0). \quad (2)$$

The post-seeding viability of yeast cells was qualitatively confirmed using scanning electron microscopy (SEM). Briefly, seeded samples were dehydrated by gradient alcohol solution and mounted onto stubs and coated in vacuum with gold before being observed through SEM (Model JEOL-6300F, Japan) at an accelerating voltage of 10 kV.

For quantitative assessment of the yeast cells' viability after being SAW treatment, a yeast suspension with identical volume to the aliquot seeded into the scaffold was pipetted onto the surface of the SAW device and subjected to SAW radiation at the input RF power applied to drive the cells into the scaffold. After being treated, aliquots of the yeast suspension were collected and diluted by adding a certain amount of culture media. The cell concentration of this suspension was counted subsequently using the haemocytometer and is defined as the cell concentration at t = 0. The yeast cells were then cultured for an additional 14 days and their concentration in the media were determined at 2, 5, 7 and 14 days. The yeast cells treated by SAW are assumed to be viable if they are able to proliferate in the prolonged culture.

2.7 Statistical analysis

All values are presented as mean ± standard deviation. Differences among experimental groups were assessed using a two-tailed Student's t-test and considered statistically significant if $p < 0.05$.

3. Results and discussion

3.1 Effect of input RF power on the particle seeding efficiency

Figure 2 shows the effect of the input RF powers on the fluid velocity and particle seeding efficiencies. The threshold power level is around 325 mW; when the input RF power is lower than this critical value, the particle seeding efficiency is very low (<50%) as there is insufficient power to drive the suspension flow into the scaffold. Most of particles were found to aggregate and deposit on the SAW substrate in this case. By increasing the input power from 325 mW to 400 mW, the particle seeding efficiency sees a sharp increase from 50% to 85% despite a slightly increase in the drop velocity to 1 mm/s. When the input power was increased to about 400 mW, however, the particle seeding efficiency appears to plateau despite continued increases in the drop velocity; with further increases in the input power, the rate at which the efficiency increases is only modest until a maximum seeding efficiency of 92% is obtained at an RF power

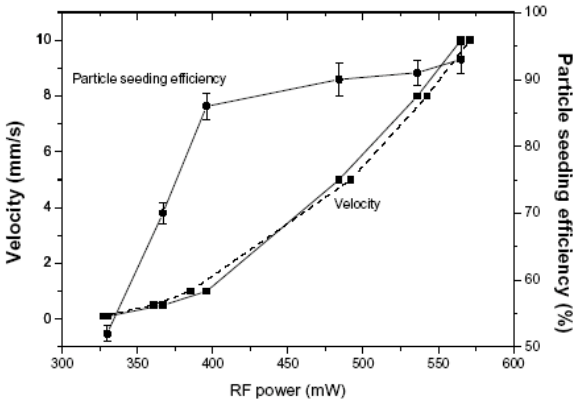

Figure 2 Effect of the input RF power on the velocity of the drop suspension prior to its contact with and entry into the scaffold, and, the particle seeding efficiency within the scaffold. The dashed line shows the quadratic relationship between velocity u and the input RF power P, as predicted by Eq. (2).

of 570 mW. Above this power level, the SAW radiation resulted in the atomisation of the drop even before it reaches the scaffold. This thus imposes an upper limit on the input RF power. Since there is no significant increase in the seeding efficiency beyond 400 mW, the subsequent experiments were conducted using this input power level.

The relationship between the velocity u and the input RF power was observed to be quadratic, which is consistent since the power P scales as

$$P \sim uF \sim \rho f R^3 u^2, \qquad (2)$$

where F is the acoustic force, ρ the density, f the SAW frequency and R the characteristic drop dimension.

3.2 Dynamics of seeding process

The dynamics of the seeding process was evaluated by analysing the high-speed video images of the particle seeding process at 400 mW. The images in the left column of Fig. 3, in which the seeding process is observed under fluoroscopic illumination, show that the SAW-driven particle seeding process is rapid. The disappearance of the fluorescence signal after 10 s indicates that approximately 85% of the particles in the initial suspension were driven into the scaffold within that time.

In contrast, when the particle suspension is allowed to perfuse into the scaffold by pure diffusion, the whole seeding process requires approximately 30 minutes, as shown in the right column of Fig. 3. Due to the small scaffold pores (roughly 200 μm), the capillary stress = γ/R_p, where γ is the surface tension and R_p is the pore dimension, is extremely large, on the order 10^2 N/m^2. As such, gravity is insufficient to drive the suspension through the scaffold and the suspension permeates the scaffold by pure diffusion alone.

3.3 Spatial distribution of seeded particles

In addition to investigating the particle seeding efficiency, the particle spatial distribution within the scaffolds was also determined in order to evaluate the uniformity of the seeding within the scaffold. By slicing the scaffold, the cross-sectional images for each slice can then be obtained through fluorescence microscopy. The first and last slices of the scaffold are shown in Fig. 4. Images in the left column show the distribution of fluorescent particles in both slices when the cell seeding process is driven by SAW actuation; the upper image shows the slice adjacent to the side where the suspension enters the scaffold whereas the bottom image shows the slice on the other end of the scaffold. This is compared to the particle distribution at the same position of a scaffold seeded by static seeding. These are shown by the images in the right column of Fig. 4 for similar slice positions.

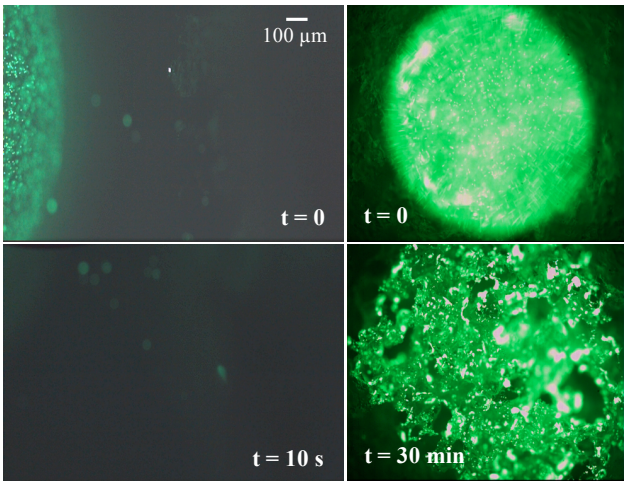

Figure 3 Seeding dynamics of the fluorescent polystyrene particles. The images in the left column show a side view of the SAW-driven perfusion process in roughly 10 s. The images in the right column show particle perfusion under the static cell seeding method, which takes significantly longer.

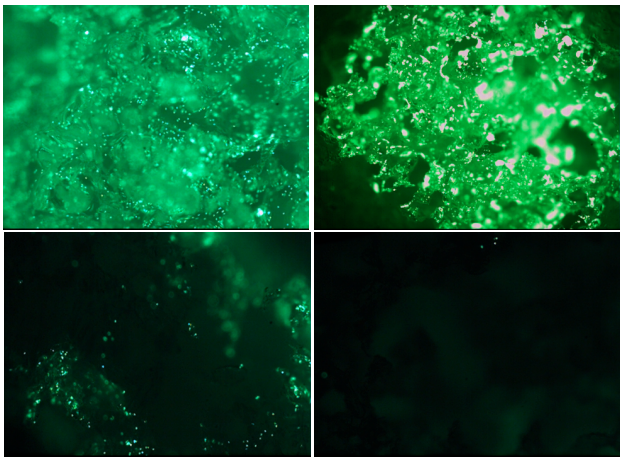

Figure 4 Scaffold cross-sectional slices showing the distribution of the cell seeding. The left column shows the first (top) and last (bottom) scaffolds slices seeded by SAW whereas the right column shows that seeded by the static method.

We thus observe that in addition to rapid cell seeding, the use of SAW actuation to drive the particle suspension into the scaffold gives both greater particle penetration into the scaffold and a more uniform particle distribution. It can be seen from Fig. 4 that more particles are in the end slice of the scaffold seeded with SAW-driven actuation compared to that with static seeding. In the static method, most of the particles remained in the surface layer; there are almost no particles in the end slice, indicating that the particles have failed to penetrate through the entire scaffold due to the inability of gravitational forces to overcome the large capillary pressure drop over the entire scaffold length. The penetration depth observed in this experiment was roughly 20% of the entire scaffold length; the fluorescence intensity was observed to drop sharply in the slices adjacent to the slice through which the drop enters (not shown).

3.4 Seeding efficiency of yeast cells

The yeast cells were seeded into the scaffold using both static and SAW-driven methods in a similar manner to that for the PS particles. Figure 5 shows the cell seeding efficiency for each 1 mm slice cut across the entire scaffold. The cell seeding efficiency in each cross-sectional slice of the scaffold seeded by the SAW method was around 20%. By comparison, 68% of the initial cells were seeded within slice *a* whereas almost no cells

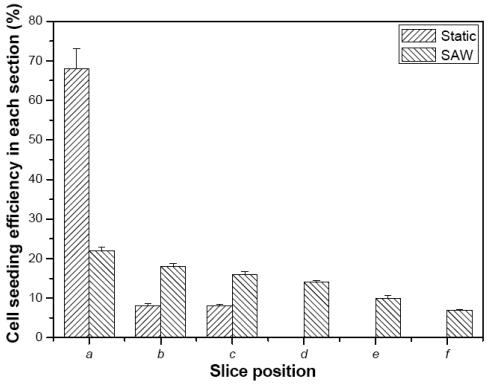

Figure 5 Yeast cell seeding efficiency in each section of the scaffold seeded by the two methods indicating that the SAW-driven seeding method produces a more uniform cell distribution within the scaffold as compared to that by the static method.

were delivered to slices $d - f$ via the static seeding method. The total cell seeding efficiencies, 87%±5% for SAW-driven seeding and 83%±5% for static seeding, however, did not yield any observable statistical differences.

3.5 Viability of yeast cells after SAW-driven seeding

Figure 6(a) shows SEM images of the porous scaffold within which yeast cells have been delivered. The yeast cells appear in the images as tiny spheroidal/ellipsoidal spots that attach themselves to the pore walls of the scaffold. A typical yeast cell is approximately equal in size to a human red blood cell and is spherical to ellipsoidal in shape. If the cells were denatured by the SAW radiation as they are driven into the pores, they would be fragmented and would appear in the images as non-homogenous particles rather than as homogeneous spheres or ellipsoids. Moreover, their sizes would appear to be much smaller and less uniform. The uniform size and shapes of the yeast cells in the SEM images therefore show that the morphology of the yeast cells seeded within the scaffolds using SAW is preserved. In addition, the yeast cells treated by SAW still maintain their ability to proliferate in the prolonged culture during the subsequent 14 days (Fig. 6(b)), further confirming that the SAW radiation at the RF powers employed does not inflict damage on the yeast cells.

4. Conclusion

A low-cost and miniaturisable alternative for driving a particle suspension into a porous scaffold using SAW actuation has been demonstrated. The method has many advantages. First, the particle/cell seeding time can be significantly shortened by several orders of magnitude. Secondly, more particles/cells can be delivered into scaffold and distributed deeper into the scaffold using SAW, thus resulting in higher seeding efficiencies as compared with the static method in which perfusion is driven by pure diffusion alone. In addition, the particles/cells can be delivered and distributed in the scaffold more uniformly by SAW actuation. More the SAW irradiation is shown to not denature or lower the viability of the yeast cells, indicating that this method has the potential to be used for cell seeding in tissue and orthopaedic engineering.

Acknowledgments

The authors would also like to thank Dr. Christopher Langendorf (Department of Biochemistry, Monash University) for providing the yeast cells.

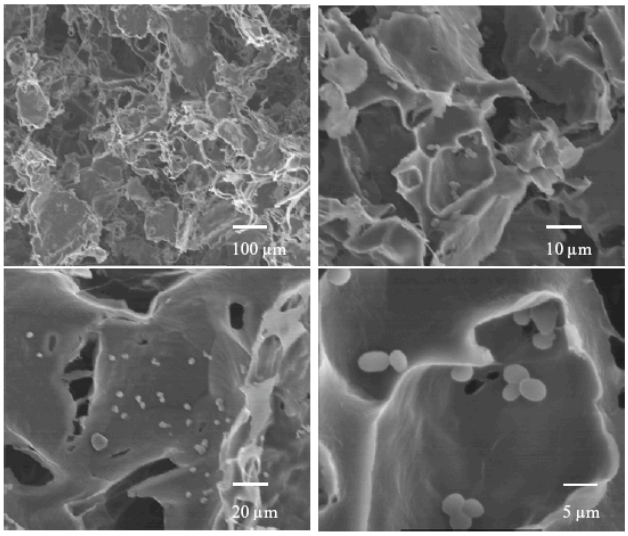

(a)

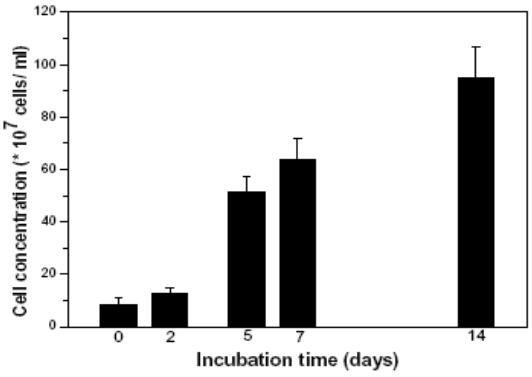

(b)

Figure 6 (a) SEM images of yeast cells seeded into the scaffolds by SAW actuation. The morphology of the cells do not appear to be compromised by the SAW treatment. (b) Proliferation rates of yeast cells after irradiation with SAWs. Cells are observed to continue proliferating during the subsequent 14 days, which further confirms the viability of the yeast cells.

References

[1] Guttenberg Z, Rathgeber A, Keller S, Radler JO, Wixforth A, Kostur M, Schindler M, Flow profiling of a surface-acoustic-wave nanopump, *Phys Rev E Stat Nonlin Soft Matter Phys* **70**, 2004, 056311.

[2] Morita T, Kurosawa MK, Higuchi T, Simulation of surface acoustic wave motor with spherical slider, *IEEE Trans Ultrason Ferroelec, Freq Contr* **46,** 1999, 929-934.

[3] Sritharan K, Strobl CJ, Schneider MF, Wixforth A, Guttenberg Z, Acoustic mixing at low Reynolds numbers, *Appl Phys Lett* **88**, 2006, 054102.

[4] Tan MK, Friend, JR, Yeo, LY, Microparticle collection and concentration via a surface acoustic wave device, *Lab Chip* **7**, 2007, 618-625.

[5] Li H, Friend JR, Yeo LY, Surface acoustic wave concentration of particle and bioparticle suspensions, *Biomed Microdev*, 2007, DOI 10.1007/s10544-007-9058-2.

[6] Wixforth A, Strobl C, Gauer Ch, Toegl A, Scriba J, Guttenberg AV, Acoustic manipulation of small droplets, *Anal Bioanal Chem* **379,** 2004, 982-991.

[7] Soletti L, Nieponice A, Guan J, Stankus JJ, William WR, Vorp DA, A seeding device for tissue engineered tubular structures, *Biomaterials* **27**, 2006, 4863-4870.

[8] Wendt D, Marsano A, Jakob M, Heberer M, Martin I, Oscillating perfusion of cell suspensions through three-dimensional scaffolds enhances cell seeding efficiency and uniformity, *Biotechnol Bioeng* **84**, 2003, 205-214.
[9] Maquet V, Martin D, Malgrange B, Franzen R, Schoenen J, Moonen G, Jerome R, Peripheral nerve regeneration using bioresorbable macroporous polylactide scaffolds, *J Biomed Mater Res* **52,** 2000, 639-651.
[10] Glicklis R, Shapiro L, Agbaria R, Merchuk J.C., Cohen S. Hepatocyte behavior within three-dimensional porous alginate scaffolds, *Biotechnol Bioeng* **67**, 2000, 344-353.
[11] Yoshikawa T, Ohgushi H, Tamai S, Immediate bone forming capability of prefabricated osteogenic hydroxyapatite, *J Biomed Mater Res* **32,** 1996, 481-492.
[12] Dong J, Uemura T, Shirasaki Y, Tateishi T, Promotion of bone formation using highly pure porous b-TCP combined with bone marrow-derived osteoprogenitor cells, *Biomaterials* **23**, 2002, 4493-4502.
[13] Li H, Friend JR, Yeo LY, A scaffold cell seeding method driven by surface acoustic waves, *Biomaterials* **28**, 2007, 4098-4104.
[14] Li H, Chang J, Preparation and characterization of bioactive and biodegradable wollastonite/Poly(D, L-lactic acid) composite scaffolds, *J Mater Sci: Mater Med* **15**, 2004, 1089-1095.
[15] Yang J, Shi GX, Bei JZ, Wang SG, Cao YL, Shang QX, Yang GG, Wang WJ. Fabrication and surface modification of macroporous poly(L-lactic acid) and poly(L-lactic-co-glycolic acid) (70/30) cell scaffolds for human skin fibroblast cell culture. *J Biomed Mater Res* **62**, 2002, 438-446.